Sustainable Chemistry

International Edition: DOI: 10.1002/anie.201603395
German Edition: DOI: 10.1002/ange.201603395

Solvent Extraction: Structure of the Liquid–Liquid Interface Containing a Diamide Ligand

*Ernesto Scoppola, Erik B. Watkins, Richard A. Campbell, Oleg Konovalov, Luc Girard, Jean-Francois Dufrêche, Geoffroy Ferru, Giovanna Fragneto, and Olivier Diat**

Abstract: *Knowledge of the (supra)molecular structure of an interface that contains amphiphilic ligand molecules is necessary for a full understanding of ion transfer during solvent extraction. Even if molecular dynamics already yield some insight in the molecular configurations in solution, hardly any experimental data giving access to distributions of both extractant molecules and ions at the liquid–liquid interface exist. Here, the combined application of X-ray and neutron reflectivity measurements represents a key milestone in the deduction of the interfacial structure and potential with respect to two different lipophilic ligands. Indeed, we show for the first time that hard trivalent cations can be repelled or attracted by the extractant-enriched interface according to the nature of the ligand.*

Interfaces between two immiscible liquids are ubiquitous in chemistry and biology and are the place of numerous physicochemical processes such as sorption,[1] solvation,[2] complexation.[3] Electron,[4] electrolyte,[2] molecule,[5] or colloid[6] transfer through the liquid interfaces are relevant for numerous domains like chemistry, electrochemistry driven solvent extraction,[7] nanoparticle synthesis,[8] or heterogeneous catalysis.[9] Discontinuities between both solvent properties yield different conformations of the solvent molecules at the interface with a break of the bulk symmetries. This loss of entropy is often related to a specific orientation of the molecules when they are polarizable and induces a region specificity for some reactions or transfer processes. The surface tension between both phases depends on the molecular interactions in this region that are different to those in the respective bulk phases and each species added to one solvent, surface active or not, will modify these interactions and then the structure as well as the dynamics of the pure liquid interface.

In solvent extraction using amphiphilic ligands or extractant molecules to separate ions, the ion partitioning between both immiscible phases is significantly enhanced by the extractant/ion complex formation on one side of the interface depending on the hydrophilicity or lipophilicity of the ligand.[10] The role of complexation (metal–ligand interaction) and supramolecular aggregation of the ligands are strongly determinant in the distribution and separation factors.[11] If the former contribution is stronger and if the complex is soluble in the phase that contains the ligand, the solute transfer from one phase to the other will be fast but its recovery will be difficult. When the equilibrium between both contributions is within a few $k_B T$[12] then hydrodynamic or interfacial factors become preponderant and have to be taken into account. Ion extraction can be referred to as a diffusion-limited or a reaction-limited process depending on the height of the energy barrier at the liquid–liquid (LL) interface.[13]

The present contribution shows that determination of the extractant and ion distributions across the water–oil interface can help the understanding of these two types of dynamics for ion transfer in a solvent extraction system. Few experimental techniques that probe a buried liquid interface, such as linear[14] and nonlinear reflection or spectroscopic optical methods or X-ray and neutron reflectivity,[15] are available to access this specific concentration profile. Although access to large facility instrumentation is required, reflectivity techniques have already demonstrated their benefit in numerous interfacial characterizations because the explored domain defined in Fourier space by the amplitude and the direction of the scattering wave vector Q fits perfectly with the nanometer range of spatial information. For these purposes, two systems were selected involving diamide ligands DMDOHEMA (or *N*,*N*′-dimethyl *N*,*N*′-dioctyl hexyl ethoxy malonamide) and DMDBTDMA (or *N*,*N*′-dimethyl-*N*,*N*′-dibutyl-2-tetradecyl-malonamide) and, which we label EXT1 and EXT2, respectively. The chemical structures of the ligands are shown in Figure 1 (upper parts). These lipophilic extractants are currently used in the nuclear industry to separate f-elements from high-level radioactive liquid waste by LL extraction processes[16] (the DIAMEX process) as well as in the more conventional field of hydrometallurgy to recycle rare-earth elements.[17] For our purpose, we have chosen to work with neodymium in its nitrate form. These extractant molecules have amphiphilic properties[18] that allow first a complexation

[*] Dr. E. Scoppola, Dr. E. B. Watkins, Dr. R. A. Campbell, Dr. G. Fragneto
Institut Laue-Langevin
38000 Grenoble (France)
Dr. E. B. Watkins
Materials Synthesis and Integrated Devices
Los Alamos National Laboratory
Los Alamos, NM 87545 (USA)
Dr. O. Konovalov
European Synchrotron Radiation Facility
38430 Grenoble (France)
Dr. G. Ferru
Argonne National Labororatory
Lemont, IL 60439 (USA)
Dr. E. Scoppola, Dr. L. Girard, Prof. J.-F. Dufrêche, Dr. O. Diat
Institut de Chimie Séparative de Marcoule
UMR 5257 CEA/CNRS/ENSCM/Université Montpellier
30207 Bagnols-sur-Cèze (France)
E-mail: olivier.diat@cea.fr

Supporting information for this article can be found under: http://dx.doi.org/10.1002/anie.201603395.

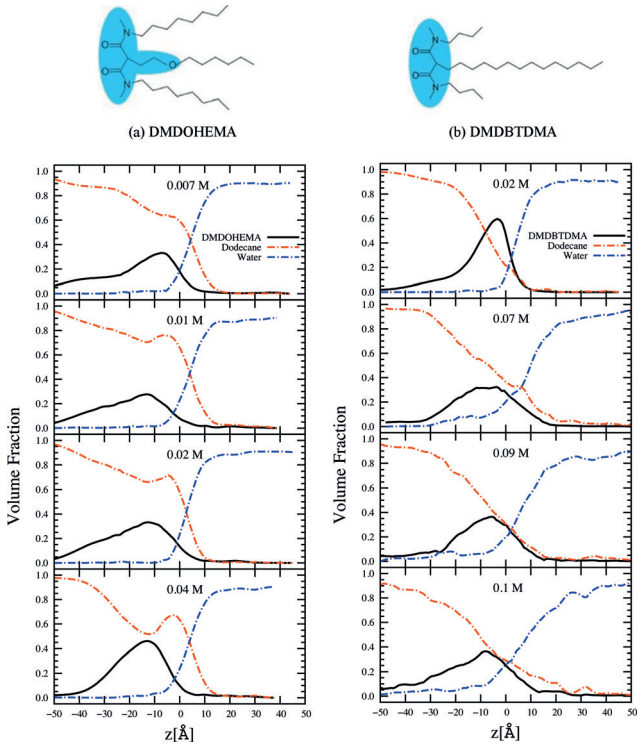

Figure 1. a) Concentration profiles across the LL interface (*z*-coordinate) of water, oil, and extractant at four concentrations of DMDOHEMA or EXT1 (0.007, 0.01, 0.02, and 0.04 mol L^{-1}) with the chemical structure of the extractant. The CAC for such a system is about 0.04 mol L^{-1}. b) Concentration profiles across the LL interface of water, oil, and extractant at four concentrations of DMDBTDMA or EXT2 (0.02, 0.07, 0.09, and 0.1 mol L^{-1}). The CAC for such a system is about 0.1 mol L^{-1}. The light blue colored region over the structures defines the polar part of the molecules.

of the ligands with specific cations at the interface, second an increase in efficiency of the emulsification that occurs during the solvent extraction process and third a structuration of the oil phase that depends on the extractant concentration and the activity of the various species in the water phase. Due to such surfactant behavior, these molecules indeed form nanoscale structures above a given critical aggregation concentration (CAC) within the organic phase such as inverted micelles or reversed aggregates.[19] For diamide in dodecane and in contact with an aqueous phase containing neodymium nitrate salt, the CAC of extractant varies between 0.01 and 0.1M depending on the diamide chemistry and the water activity.[20] In our case we worked with 0.25M of neodymium nitrate and 3M of lithium nitrate as buffer salts to fix the activity in the aqueous phase, the Li cation extraction by malonamide being negligible. Using the pendant droplet method to determine the variation of the water–oil surface tension as a function of the extractant concentration, we found a CAC of about 0.04M for EXT1 and 0.1M for EXT2 (see Figure SI.1 in the Supporting Information).

The combination of X-rays and neutrons is very helpful to understand the microscopic structure at the LL interface. X-rays reveal the distribution of higher electron density aqueous solutes (salts, nitric acid) and neutrons are the perfect probes to quantify the structuration of protonated solvents and extractant molecules thanks to the use of isotopic substitution.[21] The application of this combination to reflectivity experiments makes it possible to determine the total neutron or electron scattering length density (SLD) profile $\rho_{x,n}(z)$ across the LL interface. In the first-order Born approximation, the X-ray or neutron reflectivity is the Fourier transform of the SLD variation along the *z*-axis (see the geometry of the experiment and equation in the Materials and Methods). Using the Parratt formalism based on describing the SLD variation across the interface as a series of an arbitrary number of homogeneous layers[22] it is possible to extract from the reflectivity curves two SLD profiles that correlate with the in-plane averaged distributions of each species in solution probed by neutrons and X-rays. Using a second formalism based on a random Monte Carlo sampling (RMCS) that we have developed in Fortran code we have determined the distribution profile of each molecular species, (ions, extractant and solvent) which can be represented by the corresponding volume or molar fraction as a function of the *z*-coordinate across the water–oil interface (*z* being negative in oil and positive in water). For a given thermodynamic condition, the set of concentration profiles that match both SLD distributions within some error criteria is averaged and refined by simultaneously fitting back X-ray and neutron reflectivity data using the Parratt formalism. Some details of the experimental geometry as well as the various steps of the data analysis are given in the Material and Methods and an example is given in the Supporting Information (SI.2).

In Figure 1 the results of this analysis are plotted for two sets of reflectivity measurements (see SI.3) of the two biphasic systems described above and registered at the equilibrium state. First, only water, dodecane, and extractant concentration profiles across the LL interface are shown as a function of four extractant contents, below the CAC. On the left-hand side the main observation for the EXT1 system is an increase of the extractant adsorption at the interface when approaching the CAC as expected for a surface active molecule. Further, the data reveal that the center of mass of the extractant distribution is more inside the oil phase.[23] On the right-hand side the evolution of extractant adsorption for the EXT2 system looks rather different. At low molar content, the extractant is localized in a more defined region at the boundary between the oil and water phases, as expected for a surfactant molecule. However, with increasing extractant concentration its distribution spreads towards the aqueous phase with a center of mass of the distribution closer to the aqueous phase than observed for EXT1.

In Figure 2, the concentration profiles of the cations (Li and Nd) are plotted and compared to those of the extractants profiles for the four selected extractant concentrations. Here again, for both systems we observe different ion distributions with respect to the type of extractant. First for the EXT1 system (left plots), the ion concentration profiles both for Li and Nd are rather constant, and the ions are located exclusively in the aqueous phase (i.e. at positive *z* values). The profiles drop abruptly in the oil phase, decaying to zero within one nanometer of the interface. It is evident that there is negligible overlap between the ion and extractant profiles, hence the binding between the extractant and the ions occur

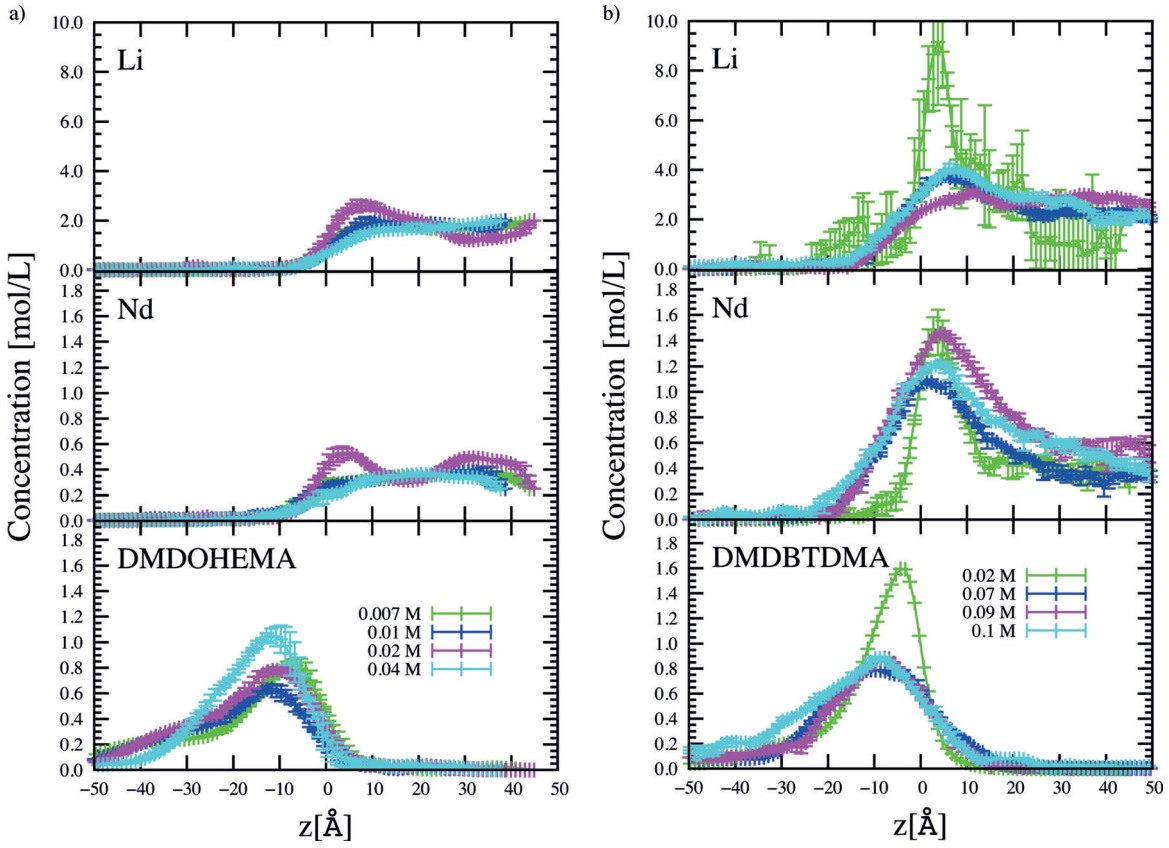

Figure 2. a) Concentration profiles in mol L^{-1} across the LL interface (*z*-coordinate) of lithium, neodymium cation and extractant at four concentrations of DMDOHEMA or EXT1 (0.007, 0.01, 0.02, and 0.04 mol L^{-1}). b) Concentration profiles across the LL interface of lithium, neodymium cations, and extractant at four concentrations of DMDBTDMA or EXT2 (0.02, 0.07, 0.09, and 0.1 mol L^{-1}). Negative values of *z* correspond to the oil phase whereas positive values correspond to the aqueous phase. The vertical lines correspond to $z=0$ and are guides for the eyes to visualize the mixing between organic and aqueous species at the interface.

at a very sharp boundary between the phases. For the EXT2 system (right plots), the underlying interactions are clearly different. The profiles of Li are still rather constant with respect to the extractant concentration, there is only a small excess at the interface compared with the bulk concentration in the aqueous phase, and there is a smooth decay towards the oil phase extending beyond 1 nm in this case; these observations differ at the lowest concentration of extractant where the profile is relatively noisy. However, for the Nd profiles a significant increase close to the interface was determined with a smooth decay towards the oil phase that largely overlaps the extractant distribution.

These results reveal that the binding conformation of EXT2 to ions at the interface involves large interpenetration of the complexed cation at the LL interface whereas they are repelled with EXT1 as expected for hard cations. Note that the NO_3 anion distribution for each extractant concentration is shown in SI.4 and does not add new information to the description of the interface; it was checked that the total charge is close to zero ($< 10^{-4}$ e^- $Å^{-3}$). In case of EXT 1, some oscillations in the ion distribution profiles are observed and we do not have any explanation. However, the difference between both systems is significant and much larger than the amplitude of these oscillations.

From the molecular distributions, the concentration ratio between Nd and EXT1 or EXT2 in the organic phase can be determined as function of the *z*-coordinate (see SI.5). This ratio is very low for the EXT1 system since there is no overlap between both distributions; whereas for the EXT2 system this ratio close to the interface ($z=0$) is between 0.3 and 1 over 2 nm within the oil phase as the bulk extractant concentration increases. With the excess of diamides observed at the interface that is on the order of 1 mol L^{-1}, the range of [Nd]/[DMDBTDMA] ratios is consistent with those measured in bulk phases at the third phase transition.[24] Indeed, it is known that at higher extractant concentrations, phase splitting in the organic phase (third phase formation) can be observed under the form of a gel-like and turbid phase between the water and an extractant-poor oil phase.[25] This transition is explained taking into account the interaction between extractant aggregates within the organic phase.[20c,26] In our system, the transition is beyond 0.1 M for EXT1 and around 0.2 M for EXT2 in the bulk organic phase. This phase transition can be characterized by the maximum of solubility of extracted solutes in the organic phase which depends on the extractant concentration and this limit seems to be achieved at the interface for the DMDBTDMA system. This is for this system, the signature of stronger Nd cation

interpenetration within a thick interfacial region enriched with extractant molecules.

Using a Poisson–Boltzmann equation as described in SI.6, from the concentration profile of Nd we can determine and compare the interfacial potential $V_{Nd}(z)$ for this cation between both systems at the CAC, as shown in Figure 3.

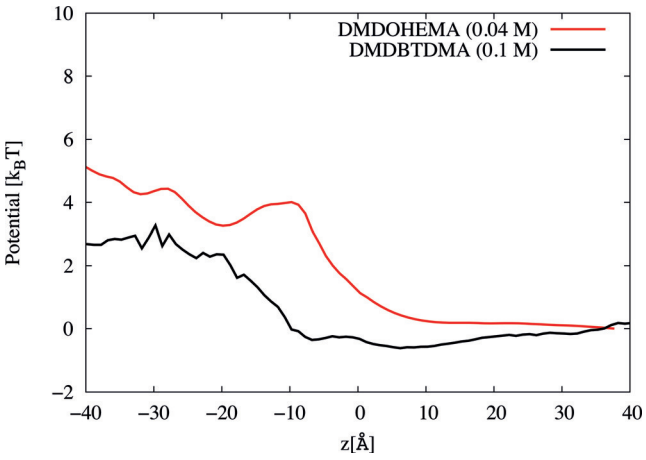

Figure 3. Interfacial potential in k_BT units across the oil–water interface for neodymium considering either DMDOHEMA or EXT1 (at 0.04 mol L^{-1}) or DMDBTDMA or EXT2 (at 0.1 mol L^{-1}). These concentrations correspond approximatively to the CAC for both systems.

Differences between the systems are evident: The energy barrier crossing the LL interface from water to oil is on the order of $4k_BT$ and is smoother for the EXT2 system with a level in oil about $2k_BT$ lower than for EXT1. Both systems are distinct in term of interfacial structuration and from this analysis it is possible to give an explanation of the different kinetics observed by Simonin et al.[13c] For both extractants we clearly observe an adsorption of the molecules at the interface with a local concentration much higher than in the bulk. In the case of DMDOHEMA, the extractant has an interfacial behaviour resembling a surfactant, consistent with its relatively low CAC. Its interfacial concentration increases with the bulk concentration and although its maximum of distribution is located more within the oil phase instead of being more highly confined at the interface as in the case of a pure oil–water interface (see SI.7), the extractant layer forms a barrier to the various cations. In the case of DMDBTDMA, we observe a thick interface that apparently allows an incursion of the hydrated pairs of ions that can be complexed by the extractant. Even though it was not possible with our approach to resolve the orientation distribution of the extractant molecules within the interfacial region, we can imagine that head to head conformation in a bi- or trilayer can exist as observed by M. Schlossman and co-workers on a different system[27] and can generate the formation of inverted micelles observed in the organic bulk phase. Of course, such structures can be formed in both systems due to thermal and hydrodynamic fluctuations, but our novel determination of the relative interfacial potential for the two systems shows that the energy barrier is weaker in the DMDBTDMA system, which favours more diffusive ion transfer.

Our data analysis still suffers from some crude assumptions such as a homogeneous distribution in the plane of the interface and approximations concerning capillary wave effects that cause thermal roughness that are not deconvoluted from the interfacial structure. However this analytical approach was equivalent for both systems which have similar surface tension variations, and therefore the comparison of the two systems has allowed us to discriminate between different structural distributions. This is static information and to move forward also we need dynamical information to report more deeply on the transfer mechanism. We worked only below and at the CAC in order not to take into account the contribution of extractant aggregation from organic bulk phases in our analysis. These low concentrations are far away from those used in industrial processes (the amount of extractant is typically in the molar range), but we can consider that the structures of the interface at higher concentrations may not differ significantly from those observed at the CAC, as the chemical potential of monomers is constant beyond this concentration. Finally it is important to note that at this Nd concentration (0.25 M), the third phase transition is closer in term of extractant concentration for DMDBTDMA than for DMDOHEMA and thus we can consider the formation of a critical adsorption that will be consistent with the cation/extractant ratio determined in the interfacial region. The organic bulk organization conditions the structure at liquid–liquid interface and we could imagine that for solvent extraction systems characterized by slow kinetics, the distance in composition to the third phase formation could be an important factor in the ion-transfer kinetics.[1]

We have also realized the novel application of these two reflectivity techniques coupling different contrasts in scattering and electron density to be able to determine the potential energy across a composite liquid interface for this type of complex systems. It was then possible for us to relate the relative energy barriers across the interface for the two extractants studied to the nature of the ion transfer and the structure of the interface. The work has also allowed us to make a link between experiments and simulation as proposed by G. Benay and G. Wipff in such systems.[28] These results should serve as a basis for further understanding the extraction mechanism, to improve the efficiency and kinetics of existing processes, and to develop new ones. These methodological developments will also allow studying other liquid interfaces (e.g. in phase transfer catalytic systems).

Acknowledgements

This work was supported by the national funding (ANR 12-BS08-0021; ILLA). The authors would like to thank ILL (grant number 9-10-1283/1350:9-12-375) and ESRF (grant number SC3766-4006) for beamtime, the SANE service at the ILL for technical support with cell building, the Partnership for Soft Condensed Matter for provision of sample preparation facilities and Yuri Gerelli for useful input during software development.

Keywords: ion transfer · liquid interfaces · neutron reflectometry · surface chemistry · X-ray reflectometry

How to cite: *Angew. Chem. Int. Ed.* **2016**, *55*, 9326–9330
Angew. Chem. **2016**, *128*, 9472–9476

[1] A. Hirtz, K. Bonkhoff, G. H. Findenegg, *Adv. Colloid Interface Sci.* **1993**, *44*, 241–281.
[2] D. Chandler, *Nature* **2005**, *437*, 640–647.
[3] M. L. Schlossman, A. M. Tikhonov, *Abstr. Pap. Am. Chem. Soc.* **2002**, *224*, U296–U296.
[4] M. Tsionsky, A. J. Bard, M. V. Mirkin, *J. Am. Chem. Soc.* **1997**, *119*, 10785–10792.
[5] a) C. Déjugnat, O. Diat, T. Zemb, *ChemPhysChem* **2011**, *12*, 2138–2144; b) P.-M. Gassin, G. Martin-Gassin, D. Meyer, J.-F. Dufreche, O. Diat, *J. Phys. Chem. C* **2012**, *116*, 13152–13160.
[6] A. Stocco, M. Chanana, G. Su, P. Cernoch, B. P. Binks, D. Wang, *Angew. Chem. Int. Ed.* **2012**, *51*, 9647–9651; *Angew. Chem.* **2012**, *124*, 9785–9789.
[7] A. Berduque, A. Sherburn, M. Ghita, R. A. W. Dryfe, D. W. M. Arrigan, *Anal. Chem.* **2005**, *77*, 7310–7318.
[8] M. A. López-Quintela, C. Tojo, M. C. Blanco, L. G. Rio, J. R. Leis, *Curr. Opin. Colloid Interface Sci.* **2004**, *9*, 264–278.
[9] L. Leclercq, A. Mouret, A. Proust, V. Schmitt, P. Bauduin, J.-M. Aubry, V. Nardello-Rataj, *Chem. Eur. J.* **2012**, *18*, 14352–14358.
[10] J. Rydberg, M. Cox, C. Musikas, G. R. Choppin, *Solvent extraction principles and practice*, Marcel Dekker, New York, **2004**.
[11] T. Zemb, C. Bauer, P. Bauduin, L. Belloni, C. Déjugnat, O. Diat, V. Dubois, J. F. Dufreche, S. Dourdain, M. Duvail, C. Larpent, F. Testard, S. Pellet-Rostaing, *Colloid Polym. Sci.* **2015**, *293*, 1–22.
[12] J. F. Dufrêche, T. Zemb, *Chem. Phys. Lett.* **2015**, *622*, 45–49.
[13] a) W. J. Albery, J. F. Burke, E. B. Leffler, J. Hadgraft, *J. Chem. Soc. Faraday Trans. 1* **1976**, *72*, 1618–1626; b) P. R. Danesi, R. Chiarizia, *Crit. Rev. Anal. Chem.* **1980**, *10*, 1–126; c) J.-P. Simonin, L. Perrigaud, K. Perrigaud, V. Trong-Hung, *Solvent Extr. Ion Exch.* **2014**, *32*, 365–377.
[14] S. Hénon, J. Meunier, *Thin Solid Films* **1993**, *234*, 471–474.
[15] J. Daillant, A. Gibaud, X-ray and Neutron Reflectivity, Principles and Applications, Vol. 770, Springer, **2009**.
[16] a) H. Dozol, C. Berthon, *Phys. Chem. Chem. Phys.* **2007**, *9*, 5162–5170; b) K. Nash, G. J. Lumetta, *Advanced separation techniques for nuclear fuel reprocessing and radiactive aste treatment*, Woodhead, Philadelphia, **2011**.
[17] a) F. Estler, G. Eickerling, E. Herdtweck, R. Anwander, *Organometallics* **2003**, *22*, 1212–1222; b) Q. Z. Tian, M. A. Hughes, *Hydrometallurgy* **1994**, *36*, 79–94.
[18] B. Abécassis, F. Testard, T. Zemb, L. Berthon, C. Madic, *Langmuir* **2003**, *19*, 6638–6644.
[19] a) C. Bauer, P. Bauduin, J. F. Dufreche, T. Zemb, O. Diat, *Eur. Phys. J. Spec. Top.* **2012**, *213*, 225–241; b) G. Ferru, D. G. Rodrigues, L. Berthon, O. Diat, P. Bauduin, P. Guilbaud, *Angew. Chem. Int. Ed.* **2014**, *53*, 5346–5350; *Angew. Chem.* **2014**, *126*, 5450–5454.
[20] a) A. Banc, P. Bauduin, B. Desbat, I. Ly, O. Diat, *J. Phys. Chem. B* **2011**, *115*, 1376–1384; b) Y. Meridiano, L. Berthon, X. Crozes, C. Sorel, P. Dannus, M. R. Antonio, R. Chiarizia, T. Zemb, *Solvent Extr. Ion Exch.* **2009**, *27*, 607–637; c) S. Nave, G. Modolo, C. Madic, F. Testard, *Solvent Extr. Ion Exch.* **2004**, *22*, 527–551.
[21] E. Scoppola, E. Watkins, G. Li Destri, L. Porcar, R. A. Campbell, O. Konovalov, G. Fragneto, O. Diat, *Phys. Chem. Chem. Phys.* **2015**, *17*, 15093–15097.
[22] L. G. Parratt, *Phys. Rev.* **1954**, *95*, 359–369.
[23] E. Scoppola, Thesis of Univ. Montpellier (Montpellier), **2015**.
[24] F. Testard, P. Bauduin, L. Martinet, B. Abecassis, L. Berthon, C. Madic, T. Zemb, *Radiochim. Acta* **2008**, *96*, 265–272.
[25] P. R. V. Rao, Z. Kolarik, *Solvent Extr. Ion Exch.* **1996**, *14*, 955–993.
[26] S. Nave, C. Mandin, L. Martinet, L. Berthon, F. Testard, C. Madic, T. Zemb, *Phys. Chem. Chem. Phys.* **2004**, *6*, 799–808.
[27] a) W. Bu, M. Mihaylov, D. Amoanu, B. Lin, M. Meron, I. Kuzmenko, L. Soderholm, M. L. Schlossman, *J. Phys. Chem. B* **2014**, *118*, 12486–12500; b) W. Bu, H. Yu, G. Luo, M. K. Bera, B. Hou, A. W. Schuman, B. Lin, M. Meron, I. Kuzmenko, M. R. Antonio, L. Soderholm, M. L. Schlossman, *J. Phys. Chem. B* **2014**, *118*, 10662–10674.
[28] a) G. Benay, G. Wipff, *J. Phys. Chem. B* **2013**, *117*, 7399–7415; b) G. Benay, G. Wipff, *J. Phys. Chem. B* **2014**, *118*, 3133–3149.

Received: April 6, 2016
Published online: June 20, 2016

